

Probing Lorentz Invariance Violation with Absorption of Astrophysical Gamma-rays by Solar Photons

JUSTIN D. FINKE¹ AND PARSHAD PATEL¹

¹*U.S. Naval Research Laboratory, Code 7653, 4555 Overlook Ave. SW, Washington, DC 20375-5352, USA*

(Dated: March 13, 2024)

ABSTRACT

We compute in detail the absorption optical depth for astrophysical γ -ray photons interacting with solar photons to produce electron positron pairs. This effect is greatest for γ -ray sources at small angular distances from the Sun, reaching optical depths as high as $\tau_{\gamma\gamma} \sim 10^{-2}$. We also calculate this effect including modifications to the absorption cross section threshold from subluminal Lorentz invariance violation (LIV). We show for the first time that subluminal LIV can lead to increases or decreases in $\tau_{\gamma\gamma}$ compared to the non-LIV case. We show that, at least in principle, LIV can be probed with this effect with observations of γ -ray sources near the Sun at $\gtrsim 20$ TeV by HAWC or LHAASO, although a measurement will be extremely difficult due to the small size of the effect.

1. INTRODUCTION

Lorentz invariance is one of the fundamental principles of special relativity. However, the violation of Lorentz invariance has been explored in various theories beyond the Standard Model, such as string theory, brane worlds, and loop quantum gravity (e.g., Amelino-Camelia et al. 1998; Kifune 1999; Amelino-Camelia & Piran 2001; Stecker & Glashow 2001; Mattingly 2005; Christiansen et al. 2006; Jacobson et al. 2006; Ellis et al. 2008). In the presence of Lorentz invariance violation (LIV), the normal relativistic dispersion relation for photons is modified as

$$E^2 - p^2c^2 = \pm E^2 \left(\frac{E}{E_{\text{LIV}}} \right)^n. \quad (1)$$

Here E_{LIV} is the energy scale, n is an integer (the order of the leading correction), and “+” represents superluminal LIV, and “−” represents subluminal LIV. For LIV brought about by quantum gravity models, it would be natural for E_{LIV} to be near the Planck Energy, $E_{\text{Planck}} = 1.2 \times 10^{28}$ eV. LIV can lead to a number of potentially observable effects (for a review see (Mattingly 2005)), including a number of astrophysically interesting effects (e.g., Sarkar 2002; Martínez-Huerta et al. 2020; Desai 2023). One is that the speed of light is no longer

constant, and is energy-dependent. Using this effect, time-of-flight experiments can be used with astrophysical γ -ray transients (such as gamma-ray bursts [GRBs] and blazars) to constrain LIV (e.g., Abdo et al. 2009; Vasileiou et al. 2013; Ellis et al. 2019). The lack of photon decay in Galactic γ -ray sources measured with HAWC has led to strong constraints on superluminal LIV (Albert et al. 2020).

Another effect is the modification of the threshold for pair production from photon-photon interactions, i.e., the process $\gamma + \gamma \rightarrow e^+ + e^-$. Subluminal LIV can be constrained with this process with γ -rays from extragalactic sources (such as blazars and GRBs), which are absorbed by ultraviolet through far-infrared photons from the extragalactic background light (EBL; e.g., Nikishov 1962; Gould & Schröder 1967a; Fazio & Stecker 1970; Franceschini et al. 2008; Razaque et al. 2009; Finke et al. 2010; Kneiske & Dole 2010; Domínguez et al. 2011; Helgason & Kashlinsky 2012; Stecker et al. 2012; Scully et al. 2014; Khaire & Srianand 2015; Stecker et al. 2016; Franceschini & Rodighiero 2017; Andrews et al. 2018; Khaire & Srianand 2019; Saldana-Lopez et al. 2021; Finke et al. 2022). The EBL is the integrated background light from all the stars that have existed in the observable universe, either through direct emission, or through absorption and re-radiation by dust. Both the EBL and the γ -ray spectra of extragalactic sources are rather uncertain. Nevertheless, after the discovery of photons out to 20 TeV from Mrk 501 by HEGRA (Aharonian et al. 1999), a number of authors suggested

justin.finke@nrl.navy.mil

parshadkp@gmail.com

LIV was needed to explain how the γ -rays at these high energies could avoid EBL absorption and reach Earth (e.g., Kifune 1999; Protheroe & Meyer 2000). Since then, studies of the $\gamma + \gamma \rightarrow e^+ + e^-$ process between extragalactic γ -ray sources and the EBL have been used to constrain LIV (e.g., Biteau & Williams 2015; Tavecchio & Bonnoli 2016; Abdalla et al. 2019; Dzhappuev et al. 2022; Baktash et al. 2022; Li & Ma 2023; Finke & Razzaque 2023). This will continue with the greatly improved sensitivity of the Cherenkov Telescope Array (CTA; Abdalla et al. 2021). Constraints have also been made from the upper limits on ultra-high energy γ -ray flux measured by the Auger Observatory (e.g., Guedes Lang et al. 2018). In this manuscript, we explore only the effect of subluminal LIV on $\gamma\gamma$ absorption.

There are (at least) two formulations of the effects of LIV on the photon-photon pair production process commonly used in the literature. One is by Jacob & Piran (2008). In their formulation, the standard model cross section formula is used, modifying only the threshold energy and the cross-section's dependence on this threshold. The other is by Fairbairn et al. (2014). Those authors define an effective mass that is related to the LIV energy scale, and use that to define an invariant center of mass energy. The two formulations *do not* give equivalent results. A comparison of the two is given by Tavecchio & Bonnoli (2016).

Another possible application of the $\gamma + \gamma \rightarrow e^+ + e^-$ process to LIV constraints could come from the extinction of astrophysical γ -ray photons by photons from the Sun. Preliminary estimates of this process were done by (Loeb 2022; Balaji 2023). Here we explore this effect in much greater detail, including its application to constraining LIV. As we will see below, subluminal LIV can make the γ -ray absorption optical depth more transparent *or more opaque* than it would be without LIV, depending on the photon distribution interacting with the γ -rays. This may allow LIV to be constrained with measurements of the γ -ray sky at energies of $\gtrsim 20$ TeV, although such measurements will be difficult to make.

In Section 2, we describe our detailed calculations of absorption of astrophysical γ -rays by solar photons, both with and without LIV included. In Section 3 we describe the potential for observing this effect and how it could be used to constrain LIV. Finally we conclude with a summary in Section 4.

2. FORMALISM

2.1. Setup

Consider an astrophysical γ -ray photon coming towards the Earth from outside the solar system. Let the

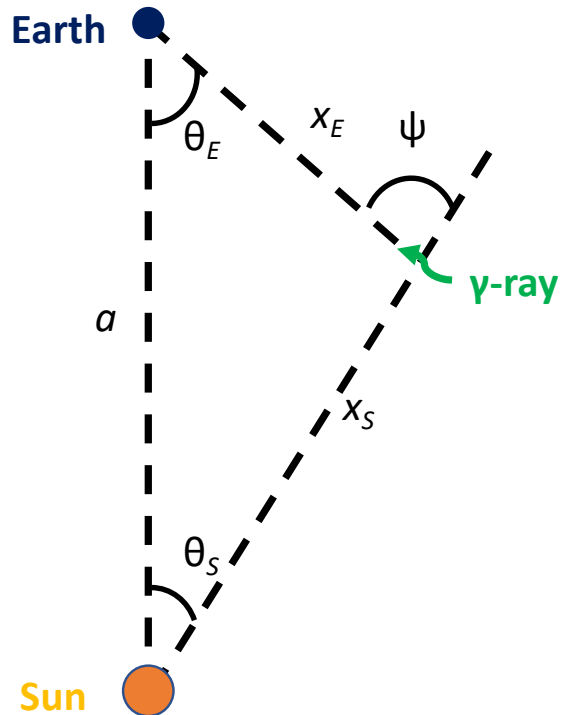


Figure 1. Geometry of solar system and γ -ray heading towards Earth. Distances and angles are labeled.

angle at the Earth between the sun and the γ -ray photon be $\theta_E \equiv \cos^{-1}(\mu_E)$; the angle at the Sun between the Earth and the γ -ray photon is $\theta_S \equiv \cos^{-1}(\mu_S)$. The distance between the Earth and the Sun is a ; the distance between the Sun and the incoming γ -ray photon is x_S ; and the distance between the Earth and the γ -ray photon is x_E . See Fig. 1 for an illustration of the geometric setup.

The γ -ray photon will interact with solar photons, annihilating the photons and producing electron-positron pairs (i.e., $\gamma + \gamma \rightarrow e^+ + e^-$). The $\gamma\gamma$ absorption cross section is (e.g., Gould & Schröder 1967b; Brown et al. 1973)

$$\sigma_{\gamma\gamma}(s) = \frac{1}{2} \pi r_e^2 (1 - \beta_{\text{cm}}^2) \left[(3 - \beta_{\text{cm}}^4) \ln \left(\frac{1 + \beta_{\text{cm}}}{1 - \beta_{\text{cm}}} \right) - 2\beta_{\text{cm}}(2 - \beta_{\text{cm}}^2) \right] \quad (2)$$

where

$$\beta_{\text{cm}} = \sqrt{1 - s^{-1}}; \quad (3)$$

\sqrt{s} is the Lorentz factor of the resulting electron and positron in their center-of-momentum frame; and $r_e = 2.817 \times 10^{-13}$ cm is the classical electron radius.

The γ -ray absorption optical depth per unit distance is given by (e.g., [Dermer & Menon 2009](#))

$$\frac{d\tau_{\gamma\gamma}(\epsilon_1)}{dx_E} = \int_0^{2\pi} d\phi \int_{-1}^1 d\mu (1 - \cos\psi) \times \int_0^\infty d\epsilon n(\epsilon, \Omega) \sigma_{\gamma\gamma} \left[\frac{\epsilon\epsilon_1(1 - \cos\psi)}{2} \right], \quad (4)$$

where ϵ_1 is the dimensionless energy of the γ -rays; ϵ is the dimensionless energy of the soft photons interacting with and absorbing the γ -rays; and $n(\epsilon, \Omega)$ is the photon density of the photon field that interacts with and absorbs the γ -rays. We use the notation where ϵ_1 and ϵ represent dimensionless photon energies, i.e. photon energies in units of the electron rest energy, $m_e c^2 = 511$ keV. Here ψ is the angle between the incoming γ -ray photon and the photon from the Sun. In general, the radiation field $n(\epsilon, \Omega)$ and the interaction angle ψ can be functions of both the polar angle (θ) and the azimuthal angle (ϕ). However, for our geometry here they are independent of ϕ . Some trigonometric effort yields

$$\cos\psi = \mu_S \mu_E - \sqrt{1 - \mu_S^2} \sqrt{1 - \mu_E^2}. \quad (5)$$

Note that [Balaji \(2023\)](#) neglect the $1 - \cos\psi$ term in Equation (4). This is the primary difference in our calculations and theirs.

The γ -ray comes from a source with intrinsic (i.e., unabsorbed) γ -ray flux $F_{\text{int}}(\epsilon_1)$. It will be observed by a detector on or orbiting the Earth with a γ -ray flux $F_{\text{obs}}(\epsilon_1) = \exp(-\tau_{\gamma\gamma}(\epsilon_1, \mu_E)) F_{\text{int}}(\epsilon_1)$.

2.2. Monochromatic Approximation for Sun

We follow the formalism of [Boettcher & Dermer \(1995\)](#); [Dermer & Menon \(2009\)](#); [Dermer et al. \(2009\)](#); [Finke \(2016\)](#) to derive formulae for the photoabsorption of astrophysical γ -rays by solar photons as a function of γ -ray photon energy (ϵ_1) and angular distance on the sky of the source from the Sun (θ_E). In spherical coordinates (R_r, θ_r, ϕ_r) are the radial distance, polar angle, and azimuthal angle, respectively, for the generic radiating medium, and $\mu_r = \cos\theta_r$. In our case the radiating medium will be the Sun.

We approximate the Sun as a point source emitting monochromatic photons with dimensionless energy $\epsilon_S = 2.7\Theta$ and luminosity $L_S = 3.846 \times 10^{33}$ ergs s $^{-1}$. Here $\Theta = k_B T_S / (m_e c^2)$ where $k_B = 1.380 \times 10^{-16}$ erg K $^{-1}$ is the Boltzmann Constant and $T_S = 5780$ K is the effective temperature of the Sun. The center of the Sun is at the origin (see Fig. 1). In this case, the emissivity of the photons emitted by the Sun is

$$\dot{n}(\epsilon, \Omega) = \frac{L_S}{m_e c^2 \epsilon_S} \frac{\delta(\epsilon - \epsilon_S) \delta(R_r - R_S)}{4\pi R_S^2}, \quad (6)$$

where $R_S = 6.98 \times 10^{10}$ cm is the radius of the Sun. The photon density at a distance x from the origin is (e.g., [Boettcher & Dermer 1995](#); [Finke 2016](#))

$$n(\epsilon, \Omega) = \frac{1}{4\pi c} \int_0^{2\pi} d\phi_r \int_{-1}^1 d\mu_r \int_0^\infty dR_r \left(\frac{R_r}{x} \right)^2 \times \dot{n}(\epsilon, \Omega) \delta(\phi_r - \phi_S) \delta(\mu_r - \mu_S). \quad (7)$$

The coordinate system is chosen so that the azimuthal angle of the sun is $\phi_S = 0$. Putting Equation (6) in Equation (7) gives

$$n(\epsilon, \Omega) = \frac{L_S}{m_e c^2 \epsilon_S c} \frac{1}{4\pi x^2} \frac{\delta(\mu - \mu_S)}{2\pi} \delta(\epsilon - \epsilon_S). \quad (8)$$

We are interested in the case where the γ -ray photon interacts with a solar photon, which occurs at $x = x_S$. Substituting Equation (8) into Equation (4) results in

$$\tau_{\gamma\gamma}(\epsilon_1, \mu_E) = \frac{L_S}{4\pi \epsilon_S m_e c^3} \int_0^\infty dx_E \frac{1 - \cos\psi}{x_S^2} \times \sigma_{\gamma\gamma} \left[\frac{\epsilon_S \epsilon_1 (1 - \cos\psi)}{2} \right], \quad (9)$$

where, from the law of cosines,

$$x_S^2 = a^2 + x_E^2 - 2ax_E \mu_E \quad (10)$$

and

$$\mu_S = \frac{a^2 + x_S^2 - x_E^2}{2ax_S}. \quad (11)$$

If $\theta_E = \pi$ then $\mu_E = -1$, $\mu_S = 1$, and the integral in Equation (9) can be performed analytically, giving

$$\tau_{\gamma\gamma}(\epsilon_1, \mu_E = -1) = \frac{L_S}{2\pi \epsilon_S m_e c^3 a} \sigma_{\gamma\gamma}(\epsilon_S \epsilon_1). \quad (12)$$

This is a factor of 2 larger than the preliminary calculation by [Loeb \(2022\)](#).

2.3. Blackbody Approximation for Sun

Now we make the more realistic assumption that, instead of emitting monochromatically, the sun emits as a blackbody. We still assume the Sun is a point source. In this case, the emissivity of photons emitted by the Sun is

$$\dot{n}(\epsilon, \Omega) = \frac{L_S}{m_e c^2 \epsilon} \frac{\delta(R_r - R_S)}{4\pi R_S^2} \frac{15}{\Theta^4 \pi^4} \frac{\epsilon^3}{\exp(\epsilon/\Theta) - 1}. \quad (13)$$

Following the same procedure as in Section 2.2, we get

$$\tau_{\gamma\gamma}(\epsilon_1, \mu_E) = \frac{L_S}{4m_e c^3} \frac{15}{\Theta^4 \pi^5} \int_0^\infty d\epsilon \frac{\epsilon^2}{\exp(\epsilon/\Theta) - 1} \times \int_0^\infty dx_E \frac{1 - \cos\psi}{x_S^2} \times \sigma_{\gamma\gamma} \left[\frac{\epsilon\epsilon_1(1 - \cos\psi)}{2} \right]. \quad (14)$$

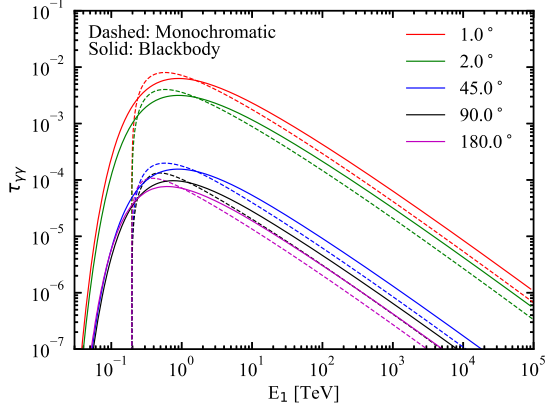


Figure 2. Absorption optical depth for astrophysical γ -rays interacting with solar photons as a function of γ -ray energy, E_1 , at different angular distances from the Sun (θ_E) as indicated by the legend. We show the monochromatic approximation (Equation [9]; dashed curves) and blackbody approximation (Equation [14]; solid curves).

Again, for $\theta_E = \pi$, the integral over x_E is analytic, so that

$$\tau_{\gamma\gamma}(\epsilon_1, \mu_E = -1) = \frac{L_S}{2m_e c^3 a} \frac{15}{\Theta^4 \pi^5} \times \int_0^\infty d\epsilon \frac{\epsilon^2}{\exp(\epsilon/\Theta) - 1} \sigma_{\gamma\gamma}(\epsilon\epsilon_1). \quad (15)$$

In Figure 2 we plot $\tau_{\gamma\gamma}$ versus γ -ray energy $E_1 = m_e c^2 \epsilon_1$ for different angles from the Sun (θ_E) for the monochromatic approximation (Equation [9]) and the blackbody approximation (Equation [14]). As one can see, the results for the monochromatic and blackbody approximations are fairly similar, although the monochromatic approximation has a hard cutoff at about 200 GeV. One cannot observe γ -ray photons that come from behind the Sun. Since the Sun has an angular diameter of $\approx 0.5^\circ$, and solar-blind γ -ray telescopes typically have angular resolutions of $\sim 1^\circ$, one could not reasonably expect to detect an astrophysical γ -ray source at an angular distance of $\theta_E \lesssim 1^\circ$ from the center of the Sun.

2.4. Lorentz Invariance Violation

Subluminal LIV can modify the threshold for the $\gamma\gamma$ absorption cross section, leading to an increase or decrease in $\tau_{\gamma\gamma}$ compared to the case without LIV. There are (at least) two ways of implementing this used in the literature, that of Jacob & Piran (2008) and Fairbairn et al. (2014). The two formulations do not give identical results.

2.4.1. Jacob & Piran Formulation

Following Jacob & Piran (2008); Biteau & Williams (2015), in the presence of subluminal LIV, Equation (9) for the monochromatic approximation becomes

$$\tau_{\gamma\gamma}(\epsilon_1, \mu_E) = \frac{L_S}{4\pi\epsilon_S m_e c^3} \int_0^\infty dx_E \frac{1 - \cos\psi}{x_S^2} \times \sigma_{\gamma\gamma} \left[\frac{\epsilon_S \epsilon_1 (1 - \cos\psi)}{2(1 + 0.25(\epsilon_1/\epsilon_{\text{LIV}})^n \epsilon_1^2)} \right], \quad (16)$$

where $\epsilon_{\text{LIV}} = E_{\text{LIV}}/(m_e c^2)$. Similarly for the blackbody approximation, Equation (14) becomes

$$\tau_{\gamma\gamma}(\epsilon_1, \mu_E) = \frac{L_S}{4m_e c^3} \frac{15}{\Theta^4 \pi^5} \int_0^\infty d\epsilon \frac{\epsilon^2}{\exp(\epsilon/\Theta) - 1} \times \int_0^\infty dx_E \frac{1 - \cos\psi}{x_S^2} \times \sigma_{\gamma\gamma} \left[\frac{\epsilon \epsilon_1 (1 - \cos\psi)}{2(1 + 0.25(\epsilon_1/\epsilon_{\text{LIV}})^n \epsilon_1^2)} \right]. \quad (17)$$

We parameterize LIV with the parameter $\xi \equiv E_{\text{LIV}}/E_{\text{Planck}}$. In Figure 3 we show $\tau_{\gamma\gamma}$ plotted versus E_1 for $\theta_E = 1^\circ$, $\theta_E = 10^\circ$ and $\theta_E = 90^\circ$ for various values of ξ in the linear ($n = 1$) LIV case. As the plot demonstrates, there is an *increase* in the gamma-ray absorption optical depth above 10 TeV, depending on the value of ξ . This is because of the LIV effect modifying the argument for $\sigma_{\gamma\gamma}$. With this modification, when sampling the cross section at energies where $0.25(\epsilon_1/\epsilon_{\text{LIV}})^n \epsilon_1^2 \gg 1$, one gets a cross section equivalent to the cross section at a lower energy. As described by Jacob & Piran (2008): “[A]t any energy above E^* [there is] an optical depth identical to the optical depth at some energy below E^* for which the pair-production threshold is the same.” In the notation of Jacob & Piran (2008), E^* is the energy above which LIV effects become important for $\gamma\gamma$ absorption. Thus, if the optical depth without LIV is *increasing* with energy, at energies where LIV is important, one will be sampling the optical depth at lower energies where $\tau_{\gamma\gamma}$ is lower, and thus one will find a *lower* $\tau_{\gamma\gamma}$ than without LIV. However, if $\tau_{\gamma\gamma}$ is *decreasing* with energy, the LIV effect allows one to sample $\tau_{\gamma\gamma}$ at a lower energy where it is higher, and thus one will find a *higher* $\tau_{\gamma\gamma}$ than without LIV.

This is demonstrated in Fig. 4 for EBL absorption. Here we plot the EBL absorption optical depth from the model of Finke et al. (2022) with no LIV, and with LIV for various values of ξ . Here the LIV effect is computed as described by Finke & Razzaque (2023), following the formulation of Jacob & Piran (2008). The dashed lines with arrows indicate the lower energies where $\tau_{\gamma\gamma}$ is being sampled for higher energies with LIV. The plot demonstrates that when $\tau_{\gamma\gamma}$ is increasing, the LIV effect causes $\tau_{\gamma\gamma}$ to be lower than it otherwise would be. But

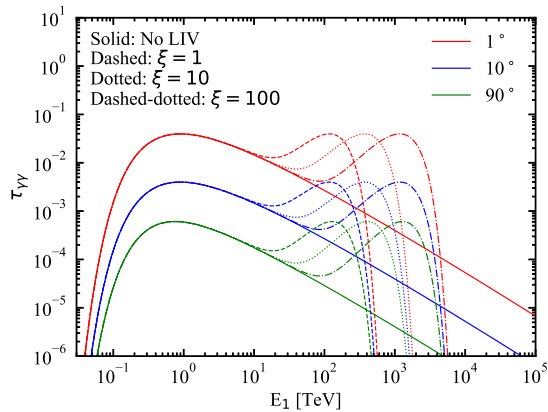


Figure 3. Absorption optical depth for astrophysical γ -rays interacting with solar photons as a function of γ -ray energy, E_1 , at different angular distances from the Sun (θ_E) as indicated by the legend, using the blackbody approximation. We show the result without LIV (solid curves; Equation [14]) and with $n = 1$ LIV using the Jacob & Piran (2008) formulation (Equation [17]) for $\xi = 1$ (dashed curves), $\xi = 10$ (dotted curves), and $\xi = 100$ (dashed-dotted curves).

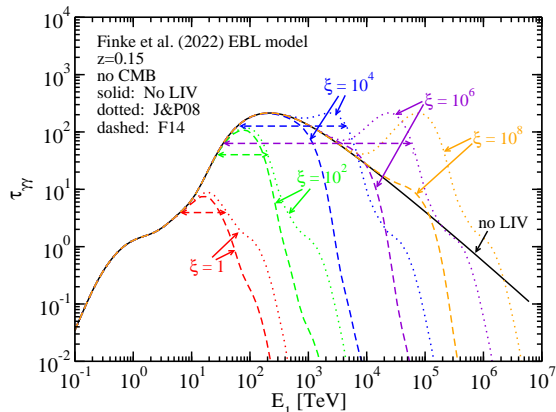


Figure 4. EBL absorption optical depth versus γ -ray energy for the EBL model of Finke et al. (2022) at $z = 0.15$. This is shown without LIV (solid curve), and with $n = 1$ LIV for the Jacob & Piran (2008) formulation (dotted curves) and Fairbairn et al. (2014) formulation (dashed curves) for various values of ξ , as shown in the plot. For the LIV curves from the Jacob & Piran (2008) formulation, the dashed lines with arrows indicate the $\tau_{\gamma\gamma}$ at lower energies where the $\tau_{\gamma\gamma}$ at higher energies are sampling, due to the LIV effect. Absorption by cosmic microwave background photons is not included in this plot.

where $\tau_{\gamma\gamma}$ is decreasing with energy, as it is here above a few hundred TeV, the LIV can cause an increase in $\tau_{\gamma\gamma}$.

In Figures 5 and 6 we plot $\tau_{\gamma\gamma}$ versus θ_E for various γ -ray energies including effects from LIV. The absorption optical depth decreases rapidly with increasing angular distance from the Sun. In most cases, the decrease in $\tau_{\gamma\gamma}$ is monotonic with angle. This is because at large x_E as

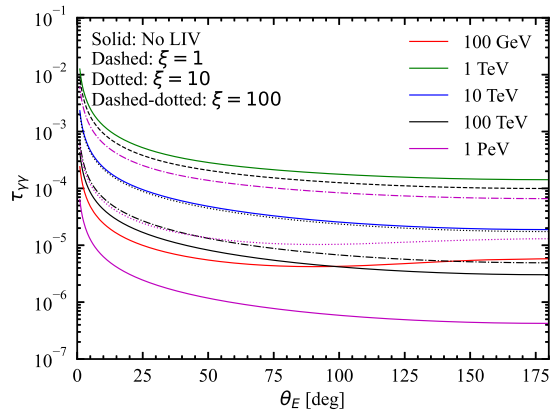


Figure 5. Absorption optical depth for astrophysical γ -rays interacting with solar photons as a function of angular distances from the Sun (θ_E), for different γ -ray energies as indicated by the legend, using the blackbody approximation. We show the result without LIV (solid curves; Equation [14]) and with $n = 1$ LIV using the Jacob & Piran (2008) formulation (Equation [17]) for $\xi = 1$ (dashed curves), $\xi = 10$ (dotted curves), and $\xi = 100$ (dashed-dotted curves). The 1 TeV curve has been scaled up by a factor of 2 and the 100 TeV $\xi = 1$ curve has been scaled up by a factor of 1.5 for clarity.

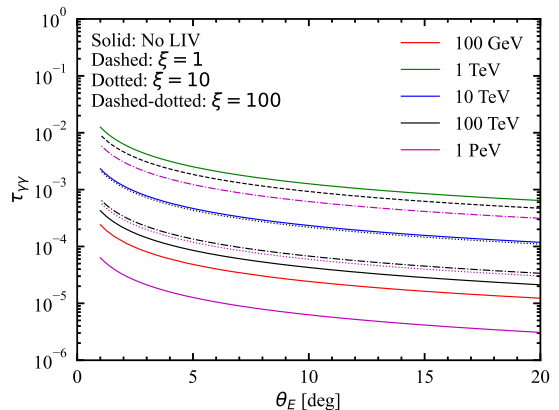


Figure 6. The same as Fig. 5, but with θ_E from 0° to 20° .

θ_E increases, the cross section argument $\epsilon_1 \epsilon (1 - \cos \psi)/2$ increases, and the cross section generally decreases with increasing energy, as long as the invariant argument is above threshold. However, the optical depth for 100 GeV decreases with increasing θ_E until it reaches a minimum at $\theta_E \approx 75^\circ$, then increases until 180° . In this case, the quantity $\epsilon_1 \epsilon (1 - \cos \psi)/2$ will go below threshold for parts of the integral over x_E for smaller θ_E . The exact results thus depend on the detailed kinematics.

For $E_1 \lesssim 10$ TeV, there is no effect of LIV on γ -ray absorption, as shown in Figures 3 and 5. For larger E_1 , the absorption optical depth will “mimic” the absorption at lower energy when LIV is included, as described

above. Thus at 1 PeV with $\xi = 10$, the result mimics the behavior of the 100 GeV curve, including the minimum at $\approx 75^\circ$. At 100 TeV for $\xi = 1$ and 1 PeV for $\xi = 10$ the results are identical to the 1 TeV curve.

2.4.2. Fairbairn et al. Formulation

Fairbairn et al. (2014) follow Protheroe & Meyer (2000) in their approach to LIV. In their formulation, the absorption optical depth for astrophysical γ -rays due to interactions with solar photons is given by

$$\begin{aligned} \tau_{\gamma\gamma}(\epsilon_1, \mu_E) &= \frac{L_S}{4\pi\epsilon_S m_e c^3} \int_0^\infty dx_E \frac{1 - \cos\psi}{x_S^2} \\ &\times \sigma_{\gamma\gamma} \left[\frac{\epsilon_S \epsilon_1 (1 - \cos\psi)}{2} - \frac{(\epsilon_1/\epsilon_{LIV})^n \epsilon_1^2}{4} \right] \end{aligned} \quad (18)$$

with the monochromatic approximation, and

$$\begin{aligned} \tau_{\gamma\gamma}(\epsilon_1, \mu_E) &= \frac{L_S}{4m_e c^3} \frac{15}{\Theta^4 \pi^5} \int_0^\infty d\epsilon \frac{\epsilon^2}{\exp(\epsilon/\Theta) - 1} \\ &\times \int_0^\infty dx_E \frac{1 - \cos\psi}{x_S^2} \\ &\times \sigma_{\gamma\gamma} \left[\frac{\epsilon \epsilon_1 (1 - \cos\psi)}{2} - \frac{(\epsilon_1/\epsilon_{LIV})^n \epsilon_1^2}{4} \right] \end{aligned} \quad (19)$$

with the blackbody approximation.

The absorption optical depth of astrophysical γ -rays with solar photons with LIV using the Fairbairn et al. (2014) formulation is shown in Fig. 7; this can be compared with the Jacob & Piran (2008) formulation plotted in Fig. 3. The Figure demonstrates that the calculation using the Fairbairn et al. (2014) formulation also can lead to an increase in the absorption optical depth relative to the calculation with no LIV, although the increase is much lower in the Fairbairn et al. (2014) formulation. This is also true for absorption of γ -rays by EBL photons, as demonstrated in Fig. 4; here again, on the region of the plot where $\tau_{\gamma\gamma}$ is decreasing with E_1 in the non-LIV case, the LIV can lead to an increase in $\tau_{\gamma\gamma}$ relative to the non-LIV case. In general, the Fairbairn et al. (2014) formulation predicts lower absorption optical depths than the Jacob & Piran (2008) formulation, as discussed by Tavecchio & Bonnoli (2016).

3. AN EXPERIMENT FOR LIV

In the preceding section, we have computed the absorption optical depth of γ -ray photons from the Sun, both with and without LIV effects included. These calculations make potentially observable predictions. The absorption is generally greatest at small angular distances from the Sun. This implies an experiment that

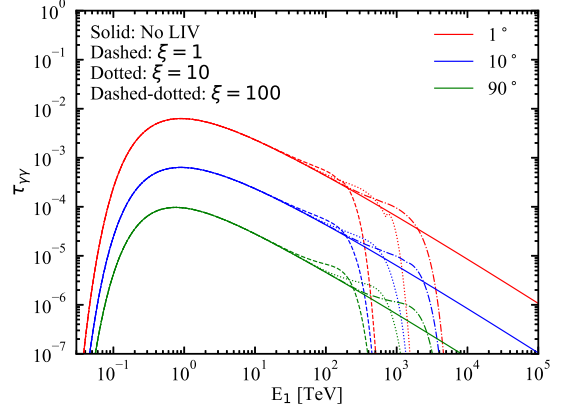


Figure 7. Same as Figure 3, but using the Fairbairn et al. (2014) formulation.

could potentially detect or constrain LIV. One would need to observe a bright γ -ray source when it is at small angular distances from the Sun, where the effect is strongest; and when it is quite far from the Sun, where the absorption is minimal. The flux near the Sun would be

$$\begin{aligned} F(\text{near}) &= F(\text{far}) \exp[-\tau_{\gamma\gamma}(\text{near})] \\ &\approx F(\text{far}) [1 - \tau_{\gamma\gamma}(\text{near})], \end{aligned} \quad (20)$$

where $F(\text{far})$ is the flux far from the Sun. The combination of these observations would give $\tau_{\gamma\gamma}(\text{near})$, the absorption optical depth near the Sun. A comparison of this with our model predictions could then constrain ξ . Assuming $F(\text{far}) \approx F(\text{near}) \approx F$ for the purposes of estimating uncertainties, and $F(\text{far})$ and $F(\text{near})$ have the same uncertainty, σ_F , standard Gaussian error propagation gives the uncertainty in $\tau_{\gamma\gamma}(\text{near})$ as

$$\sigma_{\tau_{\gamma\gamma}} = \sqrt{2} \left(\frac{\sigma_F}{F} \right). \quad (21)$$

In Fig. 8 the absorption optical depth is plotted versus ξ for $\theta_E = 2^\circ$ for a variety of photon energies. In general, observations of photons with higher energies have the greatest ability to constrain ξ . Although note there is some ambiguity; a measurement of $\tau_{\gamma\gamma} = 10^{-2}$ at 500 TeV could indicate $\xi \approx 5$ or $\xi \approx 100$. However, there are other ways to resolve these ambiguities; for instance, according to time-of-flight constraints from GRBs, $\xi \gtrsim 10$ (Vasileiou et al. 2013). To constrain LIV one must be able to observe a γ -ray source near the Sun at these very high energies. Imaging Atmospheric Cherenkov Telescopes (IACTs) such as VERITAS, H.E.S.S., MAGIC, and the upcoming CTA are not able to observe during the day and thus could not observe γ -ray sources near the Sun, but could potentially observe this effect at large angles. These leaves water Cherenkov detectors, such

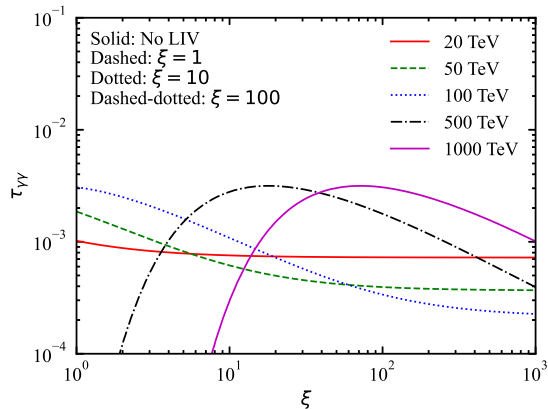


Figure 8. Absorption optical depth for astrophysical γ -rays interacting with solar photons as a function of ξ for $n = 1$ and $\theta_E = 2^\circ$, for different γ -ray energies, E_1 , as indicated by the legend, using the blackbody approximation and the Jacob & Piran (2008) formulation of LIV.

as HAWC and LHAASO. *Fermi*-LAT could potentially measure the attenuation of γ -ray photons near the Sun, but it is not sensitive at energies relevant for constraining LIV.

Compared with constraints on LIV from the EBL, the main advantage to this method is the higher degree of certainty. With EBL absorption, neither the absorbing photon source (the EBL) nor the γ -ray source spectrum is completely known (e.g., Mattingly 2005). With the experiment outlined here, the absorbing photon source

(the Sun) has a known spectrum that is approximated well by a blackbody. The γ -ray source spectrum can be known from observations when the source is not near the Sun, when absorption by this effect is negligible. The disadvantage of using the Sun is that the absorption is much smaller than with the EBL; for solar photons, $\tau_{\gamma\gamma} \sim 10^{-2}$ at most.

We estimate the possibility of detecting absorption of astrophysical photons by the Sun at 1 TeV by HAWC and LHAASO, without regard to constraining LIV. At $E_1 = 1$ TeV and $\theta_E = 2^\circ$, $\tau_{\gamma\gamma} \approx 3 \times 10^{-3}$. Assuming Poisson uncertainties and a precisely known background, $\sigma_F/F \approx \sqrt{S+B}/S$, where S and B are the source and background count rates, respectively, collected by the detector. For HAWC and LHAASO we expect $B \gg S$, so that $\sqrt{S+B}/S \approx \sqrt{B}/S$. Using Equation (21),

$$\frac{S}{\sqrt{B}} = \frac{\sqrt{2}}{\tau_{\gamma\gamma}} \left(\frac{\tau_{\gamma\gamma}}{\sigma_{\tau_{\gamma\gamma}}} \right). \quad (22)$$

For a 3σ detection, $\tau_{\gamma\gamma}/\sigma_{\tau_{\gamma\gamma}} = 3$.

One can search for the absorption of individual astrophysical γ -ray sources, or the γ -ray background. The background has the advantage of always being observable near the Sun. Its disadvantage is it is extremely faint. Indeed, the extragalactic γ -ray background has not yet been detected directly (as far as the authors know) but estimates have been made by Inoue & Tanaka (2016); Qu et al. (2019); Qu & Zeng (2022).

Table 1. VHE Sources Within 10° of the Sun.

Name	RA	Dec	Ecliptic Longitude [deg]	Ecliptic Latitude [deg]	Flux [Crab]
Sources from TevCat					
RGB J0152+017	$1^h 52^m 33^s$	$1^\circ 46' 40''$	26.78	-9.15	0.02
1ES 0229+200	$2^h 32^m 53^s$	$20^\circ 16' 21''$	42.29	4.99	0.018
RBS 0413	$3^h 19^m 47^s$	$18^\circ 45' 42''$	52.46	0.39	0.01
VER J0521+211	$5^h 21^m 45^s$	$21^\circ 12' 51''$	81.09	-1.93	0.092
Crab	$5^h 34^m 30^s$	$22^\circ 0' 44''$	84.09	-1.30	1
HAWC J0543+233	$5^h 43^m 7.2^s$	$23^\circ 24' 0.0''$	86.13	0.02	-
IC 443	$6^h 16^m 51^s$	$22^\circ 30' 11''$	93.89	-0.88	0.03
Geminga	$6^h 32^m 28^s$	$17^\circ 22' 0.0''$	97.79	-5.85	0.23
RX J0648.7+1516	$6^h 48^m 45^s$	$15^\circ 16' 12''$	101.86	-7.67	0.033
1ES 0647+250	$6^h 50^m 46^s$	$25^\circ 3' 0.0''$	101.49	2.12	0.03
2HWC J0700+143	$7^h 0^m 28^s$	$14^\circ 19' 12''$	104.80	-8.35	-
2HWC J0819+157	$8^h 19^m 55^s$	$15^\circ 47' 24''$	123.56	-3.67	-

Table 1 continued

Table 1 (*continued*)

Name	RA	Dec	Ecliptic Longitude [deg]	Ecliptic Latitude [deg]	Flux [Crab]
RBS 0723	8 ^h 47 ^m 12 ^s	11°33'50''	131.06	-6.12	0.025
OJ 287	8 ^h 54 ^m 49 ^s	20°5'58''	130.51	2.59	0.013
3C 279	12 ^h 56 ^m 11 ^s	-5°47'22''	195.17	0.20	-
2HWC J1309-054	13 ^h 9 ^m 14 ^s	-5°29'24''	198.06	1.72	-
PKS 1510-089	15 ^h 12 ^m 52 ^s	-9°6'21''	228.30	8.49	0.03
AP Librae	15 ^h 17 ^m 41 ^s	-24°22'19''	233.44	-5.94	0.02
TXS 1515-273	15 ^h 18 ^m 3.6 ^s	-27°31'34''	234.35	-8.96	0.06
HESS J1741-302	17 ^h 41 ^m 15 ^s	-30°22'37''	265.93	-7.00	0.01
HESS J1745-303	17 ^h 45 ^m 2.1 ^s	-30°22'14''	266.75	-6.97	0.05
Galactic Centre	17 ^h 45 ^m 39 ^s	-29°0'22''	266.85	-5.61	0.05
HESS J1746-308	17 ^h 46 ^m 17 ^s	-30°50'28''	267.03	-7.44	0.03
VER J1746-289	17 ^h 46 ^m 19 ^s	-28°57'58''	267.00	-5.56	-
HESS J1746-285	17 ^h 46 ^m 23 ^s	-28°52'33''	267.01	-5.47	-
MAGIC J1746.4-2853	17 ^h 46 ^m 25 ^s	-28°52'55''	267.01	-5.48	-
SNR G000.9+00.1	17 ^h 47 ^m 23 ^s	-28°9'6.0''	267.21	-4.74	0.02
Terzan 5	17 ^h 47 ^m 49 ^s	-24°48'30''	267.23	-1.40	0.015
HESS J1800-240B	18 ^h 0 ^m 26 ^s	-24°2'20''	270.10	-0.60	-
W 28	18 ^h 1 ^m 42 ^s	-23°20'6.0''	270.39	0.10	-
HESS J1800-240A	18 ^h 1 ^m 57 ^s	-23°57'43''	270.45	-0.52	-
HESS J1804-216	18 ^h 4 ^m 31 ^s	-21°42'0.0''	271.05	1.74	0.25
HESS J1808-204	18 ^h 8 ^m 37 ^s	-20°25'36''	272.02	3.00	-
HESS J1809-193	18 ^h 10 ^m 31 ^s	-19°18'0.0''	272.49	4.12	0.14
HESS J1813-178	18 ^h 13 ^m 36 ^s	-17°50'24''	273.25	5.56	0.06
2HWC J1814-173	18 ^h 14 ^m 4.8 ^s	-17°18'36''	273.38	6.09	-
SNR G015.4+00.1	18 ^h 18 ^m 4.8 ^s	-15°28'1.0''	274.40	7.90	0.018
2HWC J1819-150*	18 ^h 19 ^m 19 ^s	-15°3'36''	274.71	8.30	-
LHAASO J1825-1326	18 ^h 25 ^m 48 ^s	-13°27'0.0''	276.37	9.85	3.57
HESS J1825-137	18 ^h 25 ^m 49 ^s	-13°46'35''	276.36	9.52	0.54
2HWC J1825-134	18 ^h 25 ^m 50 ^s	-13°24'0.0''	276.38	9.90	-
LS 5039	18 ^h 26 ^m 15 ^s	-14°49'30''	276.41	8.47	0.03
1RXS J195815.6-301119	19 ^h 58 ^m 14 ^s	-30°11'11''	295.61	-9.34	-

Table 1 *continued*

Table 1 (*continued*)

Name	RA	Dec	Ecliptic Longitude [deg]	Ecliptic Latitude [deg]	Flux [Crab]
Additional Sources from LHAASO Catalog					
1LHAASO J0534+2200	5 ^h 34 ^m 26 ^s	22°3′36″	84.08	-1.25	-
1LHAASO J0542+2311	5 ^h 42 ^m 50 ^s	23°12′0.0″	86.06	-0.18	-
1LHAASO J0617+2234	6 ^h 17 ^m 24 ^s	22°35′48″	94.02	-0.78	-
1LHAASO J0634+1741	6 ^h 34 ^m 16 ^s	17°42′36″	98.20	-5.49	-
1LHAASO J0703+1405	7 ^h 3 ^m 19 ^s	14°6′0.0″	105.52	-8.49	-
1LHAASO J1809-1918	18 ^h 9 ^m 31 ^s	-20°42′0.0″	272.23	2.72	-
1LHAASO J1814-1719	18 ^h 13 ^m 4.0 ^s	-18°7′24″	273.12	5.28	-
1LHAASO J1814-1636	18 ^h 14 ^m 52 ^s	-17°23′12″	273.57	6.01	-
1LHAASO J1825-1418	18 ^h 25 ^m 9.0 ^s	-15°41′12″	276.11	7.62	-
1LHAASO J1825-1337	18 ^h 25 ^m 48 ^s	-14°23′48″	276.32	8.90	-

The advantage of individual sources is they should have many more photons than the background. The disadvantage is they do not stay near the Sun for long, since the Sun moves across the sky by approximately 1° day^{-1} . This means a point source will only be observable with 10° of the Sun for at most 20 days, so that for point sources it will be observed a fraction of the time $f_t = 0.5 \times (20 \text{ days}) / (365 \text{ days}) \approx 0.03$. We searched the TeVCat (<http://tevcat.uchicago.edu>; Wakely & Horan (2008)) for astrophysical TeV sources that get near the Sun. In Table 1 we list the TeV sources with ecliptic latitude $< 10^\circ$. As of this writing, the TeVCat has not included sources from the first LHAASO catalog (Cao et al. 2023). We included these sources in our table as well. The ecliptic latitude will be the sources’ minimum distance on the sky from the Sun. Variable sources such as blazars would not be ideal for these purposes, since one would want to compare their flux when they are near and far from the Sun. Two sources stand out as the brightest: the Crab (Aharonian et al. 2021; Cao et al. 2021a) and LHAASO J1825–1326 (Cao et al. 2021b), seen by LHAASO up to $\approx 1 \text{ PeV}$ and 500 TeV , respectively. For point sources with photon flux $\Phi_S \equiv E \, dN/dE$ the signal count rate can be approximated as

$$S \approx \Phi_S A_{\text{eff}} f_t \Delta t. \quad (23)$$

where Δt is the length of time needed to observe the source and A_{eff} is the effective area of the detector. For HAWC, we take the effective area from DeYoung & HAWC Collaboration (2012); for LHAASO we take it from Cao et al. (2019). Cosmic rays are a significant background for HAWC and LHAASO. The analysis with HAWC is able to re-

ject all but a fraction $f_r \approx 6 \times 10^{-3}$ of these cosmic rays (DeYoung & HAWC Collaboration 2012), and LHAASO can reject all but $f_r \approx 2 \times 10^{-3}$ of them (Aharonian et al. 2021). The cosmic ray background count rate is thus

$$B \approx \Phi_{\text{CR}} f_r A_{\text{eff}} f_t \Delta t \Omega, \quad (24)$$

where Φ_{CR} is the $E \, dN/dE$ cosmic ray intensity and Ω is the solid angle around the source. We take Φ_{CR} from Chapter 29 of Tanabashi et al. (2018). For HAWC and LHAASO, with angular resolution of about $\theta_{\text{psf}} \approx 1^\circ$, $\Omega \approx \pi \theta_{\text{psf}}^2 \approx 10^{-3} \text{ sr}$. For a precisely known background, the number of counts above background is

$$\frac{S}{\sqrt{S+B}} \approx \frac{S}{\sqrt{B}} \approx \frac{\Phi_S}{\sqrt{\Phi_{\text{CR}} f_r}} \sqrt{\frac{A_{\text{eff}} f_t \Delta t}{\Omega}}. \quad (25)$$

Combining Equations (22) and (25) gives the time needed for a detection,

$$\Delta t \approx \frac{2}{\tau_{\gamma\gamma}^2} \left(\frac{\tau_{\gamma\gamma}}{\sigma_{\tau_{\gamma\gamma}}} \right)^2 \frac{\Phi_{\text{CR}} f_r}{\Phi_S^2} \frac{\Omega}{A_{\text{eff}} f_t}. \quad (26)$$

Here we estimate the time for detection for the Crab and LHAASO J1825–1326 at 1 TeV. The results are in Table 2. In all cases, it would take > 30 years to make a detection. Note that although LHAASO J1825–1326 is listed as brighter than the Crab in Table 1, the energy ranges here are different, so they are not directly comparable. For the LHAASO J1825–1326 at 1 TeV listed in Table 2, we have extrapolated the power-law spectrum from Cao et al. (2021b) to lower energies.

Next we look at whether *Fermi*-LAT could detect this effect. This is complicated by the fact that for

Table 2. Detection of $\tau_{\gamma\gamma}$ at 1 TeV by VHE γ -ray instruments.

	Crab	LHAASO J1825–1326
Φ_S [$\text{cm}^{-2} \text{s}^{-1}$]	4×10^{-11}	1.5×10^{-11}
Φ_{CR} [$\text{cm}^{-2} \text{s}^{-1} \text{srad}^{-1}$]	1.4×10^{-5}	1.4×10^{-5}
$\tau_{\gamma\gamma}(\theta_E = 2^\circ)$	3×10^{-3}	3×10^{-3}
HAWC f_r	6×10^{-3}	6×10^{-3}
HAWC A_{eff} [km^2]	0.02	0.02
HAWC Δt [year]	560	4000
LHAASO f_r	2×10^{-3}	2×10^{-3}
LHAASO A_{eff} [km^2]	0.1	0.1
LHAASO Δt [year]	37	260

the LAT the Sun has a γ -ray halo around it extending for $\approx 20^\circ$ caused by the Compton scattering of solar photons by cosmic ray electrons (Moskalenko et al. 2006; Orlando & Strong 2007, 2008; Abdo et al. 2011; Linden et al. 2022). The extragalactic gamma-ray background (EGB; Ackermann et al. 2015) becomes brighter than this halo at about 5° ; we will assume the $\tau_{\gamma\gamma}$ at $\theta_E = 10^\circ$, although the exact details will likely not effect our conclusions. We use the LAT’s Pass 8 on-axis instrument response function¹. The LAT is a sky survey instrument that sees the entire sky every 3 hours with a field of view of approximately 20% of the sky. So we take $f_t = 0.2 \times 20/365 = 0.01$ for point sources. The LAT has an anti-coincidence detector to veto cosmic rays, so that at high energies it is signal dominated ($S \gg B$), and $\sigma_F/F \approx \sqrt{S+B}/S \approx \sqrt{S}/S = 1/\sqrt{S}$. This leads to

$$\Delta t \approx \frac{2}{\Phi_S A_{\text{eff}} f_t \tau_{\gamma\gamma}^2} \left(\frac{\tau_{\gamma\gamma}}{\sigma_{\tau_{\gamma\gamma}}} \right)^2. \quad (27)$$

For individual sources, we searched the *Fermi*-LAT Third Hard Source Catalog (Ajello et al. 2017) for sources with ecliptic latitude $< 10^\circ$, i.e., sources that get within 10 degrees of the Sun, and found 253 sources. Using Equation (27), we determine the total count rate for all of these sources for three energy bins given in the catalog: the 50-150 GeV, 150-500 GeV, and 500-2000 GeV bins. These results are in Table 3. Even a stacking analysis of all hard LAT sources will not detect this effect in the likely lifetime of the *Fermi* spacecraft. Further, most of these sources are blazars, which are often highly variable in γ -rays, and so would not be appropriate for this sort of measurement.

If HAWC or LHAASO could reject cosmic rays like the LAT, we could follow the same procedure for those experiments as we did for the LAT. In that case we estimate HAWC and LHAASO would be able to detect this effect in the Crab at 1 TeV in 6.5 and 1.3 years, respectively. Distinguishing between cosmic rays and photons is the strongest limitation on these experiments.

The prospects for detecting the absorption of γ -rays by solar photons at 1 TeV are poor. Higher energies are more interesting from the point of view of constraining LIV, but prospects are even worse here, since fewer photons are detected. We note that our approximation in this section is rather imprecise; we neglect all but Poisson uncertainties, and our approximations for source and background counts (Equations (23) and (24)) do not properly integrate over energy. However they are good enough for the order of magnitude level estimates provided here.

4. SUMMARY

In this paper:

- We compute in detail the effect of absorption of astrophysical γ -ray sources by solar photons, a process for which preliminary calculations were made by Loeb (2022); Balaji (2023).
- We show the absorption effect is greatest for γ -ray sources at small angular distances from sun, reaching as high as $\tau_{\gamma\gamma} \sim 10^{-2}$. As pointed out by Loeb (2022), this effect causes the γ -ray background at $\gtrsim 100$ GeV to have a greater anisotropy than the cosmic microwave background from the solar system’s motion relative to the cosmic frame. Unfortunately, the EGB is $\sim 10^6$ fainter than the CMB (e.g., Hauser & Dwek 2001), making the anisotropy much more difficult to detect.

¹ https://www.slac.stanford.edu/exp/glast/groups/canda/lat_Performance.htm

Table 3. Detection of $\tau_{\gamma\gamma}$ by *Fermi*-LAT 3FHL sources.

	50-150 GeV	150-500 GeV	500-2000 GeV
Φ_S	3.9×10^{-9}	9.9×10^{-10}	2.3×10^{-10}
$\tau_{\gamma\gamma}(\theta_E = 10^\circ)$	2.4×10^{-5}	3.8×10^{-4}	6.3×10^{-4}
A_{eff} [cm ²]	9000	9000	9000
Δt [year]	3×10^9	4×10^7	7×10^7

- We make calculations for this effect that include subluminal LIV. For the first time, we show that subluminal LIV can lead to a decrease or increase in the absorption optical depth from the pair production process compared to the non-LIV case, depending on the spectrum of the absorbing photon source. This is true for both the [Jacob & Piran \(2008\)](#) and [Fairbairn et al. \(2014\)](#) formulation of LIV. The [Jacob & Piran \(2008\)](#) formulation predicts higher values of $\tau_{\gamma\gamma}$ than the [Fairbairn et al. \(2014\)](#) one.
- We show that this effect is unlikely to be observed with water Cherenkov observatories like HAWC or LHAASO. These can observe near the Sun, unlike IACTs, but the difficulties in separating γ -rays and hadrons means the needed precision will not

be reached in a reasonable amount of time. However, a clever stacking analysis may lead to a possible detection of the effect in a more reasonable amount of time.

- 1 We are grateful to the referee for comments that
- 2 have improved this paper. We would like to thank
- 3 Teddy Cheung for pointing out there are sources in the
- 4 LHAASO catalog that are not in the TeVCat at the
- 5 time of this writing; and Brian Humensky for useful dis-
- 6 cussions on the observation of the effect described in
- 7 this manuscript. The authors were supported by NASA
- 8 through contract S-15633Y. J.D.F. was also supported
- 9 by the Office of Naval Research.

REFERENCES

- Abdalla, H., Aharonian, F., Ait Benkhali, F., et al. 2019, *ApJ*, 870, 93
- Abdalla, H., Abe, H., Acero, F., et al. 2021, *Journal of Cosmology and Astro-Particle Physics*, 2021, 048
- Abdo, A. A., Ackermann, M., Ajello, M., et al. 2009, *Nature*, 462, 331
- . 2011, *ApJ*, 734, 116
- Ackermann, M., Ajello, M., Albert, A., et al. 2015, *ApJ*, 799, 86
- Aharonian, F., An, Q., Axikegu, et al. 2021, *Chinese Physics C*, 45, 085002
- Aharonian, F. A., Akhperjanian, A. G., Barrio, J. A., et al. 1999, *A&A*, 349, 11
- Ajello, M., Atwood, W. B., Baldini, L., et al. 2017, *ApJS*, 232, 18
- Albert, A., Alfaro, R., Alvarez, C., et al. 2020, *PhRvL*, 124, 131101
- Amelino-Camelia, G., Ellis, J., Mavromatos, N. E. and Nanopoulos, D. V., & Sarkar, S. 1998, *Nature*, 393, 763
- Amelino-Camelia, G., & Piran, T. 2001, *PhRvD*, 64, 036005
- Andrews, S. K., Driver, S. P., Davies, L. J. M., Lagos, C. d. P., & Robotham, A. S. G. 2018, *MNRAS*, 474, 898
- Baktash, A., Horns, D., & Meyer, M. 2022, arXiv e-prints, arXiv:2210.07172
- Balaji, S. 2023, *Physics Letters B*, 845, 138157
- Biteau, J., & Williams, D. A. 2015, *ApJ*, 812, 60
- Boettcher, M., & Dermer, C. D. 1995, *A&A*, 302, 37
- Brown, R. W., Hunt, W. F., Mikaelian, K. O., & Muzinich, I. J. 1973, *PhRvD*, 8, 3083
- Cao, Z., della Volpe, D., Liu, S., et al. 2019, arXiv e-prints, arXiv:1905.02773
- Cao, Z., Aharonian, F., An, Q., et al. 2021a, *Science*, 373, 425
- Cao, Z., Aharonian, F. A., An, Q., et al. 2021b, *Nature*, 594, 33
- Cao, Z., Aharonian, F., An, Q., et al. 2023, arXiv e-prints, arXiv:2305.17030
- Christiansen, W. A., Ng, Y. J., & van Dam, H. 2006, *PhRvL*, 96, 051301
- Dermer, C. D., Finke, J. D., Krug, H., & Böttcher, M. 2009, *ApJ*, 692, 32

- Dermer, C. D., & Menon, G. 2009, High Energy Radiation from Black Holes: Gamma Rays, Cosmic Rays, and Neutrinos
- Desai, S. 2023, arXiv e-prints, arXiv:2303.10643
- DeYoung, T., & HAWC Collaboration. 2012, Nuclear Instruments and Methods in Physics Research A, 692, 72
- Domínguez, A., et al. 2011, MNRAS, 410, 2556
- Dzhappuev, D. D., Afashokov, Y. Z., Dzaparova, I. M., et al. 2022, The Astronomer's Telegram, 15669, 1
- Ellis, J., Konoplich, R., Mavromatos, N. E., et al. 2019, PhRvD, 99, 083009
- Ellis, J., Mavromatos, N. E., & Nanopoulos, D. V. 2008, Physics Letters B, 665, 412
- Fairbairn, M., Nilsson, A., Ellis, J., Hinton, J., & White, R. 2014, JCAP, 2014, 005
- Fazio, G. G., & Stecker, F. W. 1970, Nature, 226, 135
- Finke, J. D. 2016, ApJ, 830, 94
- Finke, J. D., Ajello, M., Domínguez, A., et al. 2022, ApJ, 941, 33
- Finke, J. D., & Razzaque, S. 2023, ApJL, 942, L21
- Finke, J. D., Razzaque, S., & Dermer, C. D. 2010, ApJ, 712, 238
- Franceschini, A., & Rodighiero, G. 2017, A&A, 603, A34
- Franceschini, A., Rodighiero, G., & Vaccari, M. 2008, A&A, 487, 837
- Gould, R. J., & Schröder, G. P. 1967a, Physical Review, 155, 1408
- . 1967b, Physical Review, 155, 1404
- Guedes Lang, R., Martínez-Huerta, H., & de Souza, V. 2018, ApJ, 853, 23
- Hauser, M. G., & Dwek, E. 2001, ARA&A, 39, 249
- Helgason, K., & Kashlinsky, A. 2012, ApJL, 758, L13
- Inoue, Y., & Tanaka, Y. T. 2016, ApJ, 818, 187
- Jacob, U., & Piran, T. 2008, PhRvD, 78, 124010
- Jacobson, T., Liberati, S., & Mattingly, D. 2006, Annals of Physics, 321, 150
- Khaire, V., & Srikanand, R. 2015, ApJ, 805, 33
- . 2019, MNRAS, 484, 4174
- Kifune, T. 1999, ApJL, 518, L21
- Kneiske, T. M., & Dole, H. 2010, A&A, 515, A19
- Li, H., & Ma, B.-Q. 2023, Astroparticle Physics, 148, 102831
- Linden, T., Beacom, J. F., Peter, A. H. G., et al. 2022, PhRvD, 105, 063013
- Loeb, A. 2022, Research Notes of the American Astronomical Society, 6, 148
- Martínez-Huerta, H., Lang, R. G., & de Souza, V. 2020, Symmetry, 12, 1232
- Mattingly, D. 2005, Living Reviews in Relativity, 8, 5
- Moskalenko, I. V., Porter, T. A., & Digel, S. W. 2006, ApJL, 652, L65
- Nikishov, A. I. 1962, JETP, 393, 14
- Orlando, E., & Strong, A. W. 2007, Ap&SS, 309, 359
- . 2008, A&A, 480, 847
- Protheroe, R. J., & Meyer, H. 2000, Physics Letters B, 493, 1
- Qu, Y., Zeng, H., & Yan, D. 2019, MNRAS, 490, 758
- Qu, Y.-k., & Zeng, H.-d. 2022, ChA&A, 46, 42
- Razzaque, S., Dermer, C. D., & Finke, J. D. 2009, ApJ, 697, 483
- Saldana-Lopez, A., Domínguez, A., Pérez-González, P. G., et al. 2021, MNRAS, 507, 5144
- Sarkar, S. 2002, Modern Physics Letters A, 17, 1025
- Scully, S. T., Malkan, M. A., & Stecker, F. W. 2014, ApJ, 784, 138
- Stecker, F. W., & Glashow, S. L. 2001, Astroparticle Physics, 16, 97
- Stecker, F. W., Malkan, M. A., & Scully, S. T. 2012, ApJ, 761, 128
- Stecker, F. W., Scully, S. T., & Malkan, M. A. 2016, ApJ, 827, 6
- Tanabashi, M., Hagiwara, K., Hikasa, K., et al. 2018, PhRvD, 98, 030001
- Tavecchio, F., & Bonnoli, G. 2016, A&A, 585, A25
- Vasileiou, V., Jacholkowska, A., Piron, F., et al. 2013, PhRvD, 87, 122001
- Wakely, S. P., & Horan, D. 2008, in International Cosmic Ray Conference, Vol. 3, International Cosmic Ray Conference, 1341–1344